Applied Physics Letters

RESEARCH ARTICLE | AUGUST 08 2023

Deformation insensitive thermal conductance of the designed Si metamaterial

Lina Yang ; Quan Zhang ; Gengkai Hu ; Nuo Yang

Appl. Phys. Lett. 123, 062201 (2023)
https://doi.org/10.1063/5.0158794

Applied Physics Letters ARTICLE pubs.aip.org/aip/apl

Deformation insensitive thermal conductance of the designed Si metamaterial

Cite as: Appl. Phys. Lett. **123**, 062201 (2023); doi: 10.1063/5.0158794
Submitted: 17 May 2023 · Accepted: 14 July 2023 ·
Published Online: 8 August 2023

Lina Yang,[1] Quan Zhang,[2] Gengkai Hu,[1] and Nuo Yang[3,a)]

AFFILIATIONS

[1]School of Aerospace Engineering, Beijing Institute of Technology, Beijing 100081, China
[2]School of Mathematical and Statistical Sciences, University of Galway, University Road, Galway H91 TK33, Ireland
[3]School of Energy and Power Engineering, Huazhong University of Science and Technology, Wuhan 430074, China

[a)]Author to whom correspondence should be addressed: nuo@hust.edu.cn

ABSTRACT

The thermal management has been widely focused due to its broad applications. Generally, the deformation can largely tune the thermal transport. The main challenge of flexible electronics/materials is to maintain thermal conductance under large deformation. This work investigates the thermal conductance of a nano-designed Si metamaterial constructed with curved nanobeams by molecular dynamics simulation. Interestingly, it shows that the thermal conductance of the nano-designed Si metamaterial is insensitive under a large deformation (strain $\sim -41\%$). The new feature comes from the designed curved nanobeams, which exhibit a quasi-zero stiffness. Further calculations show that, when under large deformation, the average stress in nanobeam is ultra-small (<151 MPa), and its phonon density of states are little changed. This work provides valuable insight on the multifunction, such as both stable thermal and mechanical properties, of nano-designed metamaterials.

Rationally designed metamaterials by the advanced fabrication techniques[1,2] have attracted great attention due to their new functionality, such as high strength/stiffness to weight ratio,[3] recoverability under strain,[2] low thermal conductivity,[4–8] damage resistance,[9] and quasi-zero-stiffness.[10] Designing nanostructured metamaterials is of great importance to achieve unprecedented multifunction.

The thermal properties of metamaterials can be severely suppressed by designing nanoscale structures, which benefits applications in phononics, thermoelectrics, thermal insulations, etc.[11,12] However, most nanostructured metamaterials are designed relatively simple in morphology, such as nanomesh,[5] phononic crystal,[7] and nanophononics with local resonators.[8] Designing morphologies of nanostructures provides new degrees of freedom to manipulate thermal properties.[13–16] For example, curved nanostructures, like kinked/bent nanowires and nanoribbon, can cause large modulation of thermal conductivity (κ).[15,17–21] Moreover, designing a film with a wavy-structure can endow a rigid film with flexibility.[22,23] Therefore, the thermal properties of metamaterial with designed morphology needs further investigation.

A deformation or strain is inevitable for devices in practical applications. Especially, flexible electronics and devices involve large deformation. Therefore, it is demanded that metamaterials possess stable thermal and mechanical properties under large deformation.[24] However, many investigations found that the deformation has an obvious effect on κ of nanostructures.[25–31] Only a few works reported an insensitive κ under a smaller deformation (strain <1%).[32,33] It is less studied that nanostructured metamaterials have insensitive κ under a larger deformation.

The question we address here is whether a nanostructured metamaterial with designed morphology can have both stable mechanical properties and thermal properties under deformation. Here, a metamaterial with designed curved Si nanobeams (DCSiNBs) is studied with a large deformation (strain $\sim -41\%$) by nonequilibrium molecular dynamics (NEMD). The deformation effect on thermal conductance (σ) is systematically investigated. Furthermore, the stress and phonon density of states (DOS) are calculated to understand the underlying mechanism.

The designed Si metamaterial is constructed by periodic arrangement of the unit cell (shown in the red dashed rectangular) in Fig. 1(a). The unit cell without deformation has length (L) of 347.6 Å and height (H) of 114.1 Å in y and x directions, respectively. The unit cell is built with DCSiNBs (shown in the blue dashed rectangular). DCSiNBs have a thickness of 10.9 Å (denoted as DCSiNB-I). The deformed Si metamaterial is constructed by the deformed unit cell

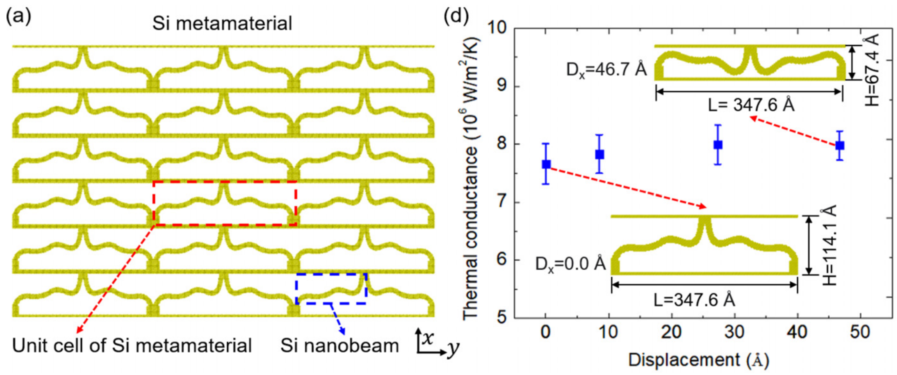

FIG. 1. (a) The structure of the designed Si metamaterial. The designed Si metamaterial is constructed by periodic arrangement of the unit cell (shown in the red dashed rectangular). DCSiNBs have a thickness of 10.9 Å (denoted as DCSiNB-I). The generation of DCSiNBs in simulation is shown in Fig. S1 in the supplementary material. (b) The thermal conductance of the deformed Si metamaterial vs the displacement of the top end of the unit cell from 0.0 to 46.7 Å at 300 K in the $-x$ direction. The insets show the structure of the unit cell of the designed Si metamaterial without deformation ($D_x = 0.0$ Å) and with a deformation ($D_x = 46.7$ Å).

with deformed DCSiNB. The deformation is described by the displacement (D_x) of top end of the unit cell in the $-x$ direction. The generation of the DCSiNB with quasi-zero stiffness (QZS) and the procedure to obtain the deformed DCSiNB are shown in Fig. S1 in the supplementary material.

The thermal conductance of the designed Si metamaterial in the x direction is calculated by the NEMD method using one unit cell by LAMMPS.[34] The fixed boundary conditions are applied in the x direction, and periodic boundary condition is applied in y and z directions. The size of the unit cell in the z direction is set as 32.6 Å to obtain converged σ. The interaction between Si atoms are described by Stillinger–Weber potential,[35] which has been widely applied in Si nanostructures. Langevin heat baths[36] with temperature of 310 and 290 K are applied at the two ends of the unit cell in the x direction, respectively. The time step of NEMD simulation is set as 0.5 fs. In the beginning, the simulation runs 4 ns to reach a steady state. Then, the simulation runs 5 ns to get an averaged heat flux and temperature profile. The structure of the designed Si metamaterial is largely deformed by compression; however, the distance of heat path is hardly changed (the length of the DCSiNBs along the axial direction). To take into account the designed feature, the thermal conductance is used in this work, which is calculated as

$$\sigma = -\frac{J}{A \cdot \Delta T}, \tag{1}$$

where J is the total heat current, A is the cross section area of the unit cell, and ΔT is the temperature difference between the two ends. The final results of σ are averaged over six simulations with different initial conditions. The error bar is the standard deviation of the six simulations.

The dependence of thermal conductance of the designed Si metamaterial on the displacement of top end of the unit cell from 0.0 to 46.7 Å is shown in Fig. 1(b). The thermal conductance calculated using two unit cell of the designed Si metamaterial is shown in Fig. S9 in the supplementary material. Interestingly, the σ along the x direction is insensitive to the large deformation (strain $\sim -41\%$), which is different from the strain effect on Si nanowire and Si film.[30] This result indicates that the designed Si metamaterial can provide a stable thermal property when working under deformation conditions.

The deformation of the designed Si metamaterial is determined by its unit cell and the behavior of DCSiNBs. Therefore, the thermal transport behavior of the deformed DCSiNBs is studied in detail. The deformed DCSiNB-I with $D_x = 0.0$, 27.3, and 46.7 Å are shown in Fig. 2(a). In addition, the force-displacement curve of the deformed DCSiNB-I is calculated in Fig. S2 in the supplementary material, which indicates the QZS feature of DCSiNBs.

The σ and temperature profile of the DCSiNB-I in the x direction is shown in Figs. 2(c) and 2(b). The structure of the corresponding straight Si beam of DCSiNB-I is shown in Fig. S6(a), which has the same thickness and number of atoms as DCSiNB-I. The temperature distributions in both x and y directions are calculated in Fig. S6 in the supplementary material. The σ of the DCSiNB-I without deformation ($D_x = 0.0$ Å) is reduced by 15.8% compared to that of the straight beam without compression (black dashed line); however, it is insensitive to the deformation as the displacement increases, which produces the same trend as that of the designed Si metamaterial.

To further understand the underlying mechanisms, DOS of the deformed DCSiNB-I with $D_x = 0$, 27.32, and 46.67 Å and the straight Si beam are calculated by the general utility lattice program (GULP)[37] in Fig. 2(d). The local DOS of atoms in DCSiNB-I are also calculated in Fig. S7 in the supplementary material. The DOS peaks of the DCSiNB-I are much smaller than that of the straight Si beam when the frequency is between 3.5 and 14 THz. Moreover, the DOS of DCSiNB-I is almost unchanged as the deformation increases, which indicates that the distribution of modes in DCSiNB-I is little affected and can cause the deformation insensitive σ of DCSiNB.

To investigate if the size of the DCSiNB can affect the thermal transport behavior under deformation, a thicker DCSiNB [denoted as DCSiNB-II in Fig. 3(a)] whose size doubles that of DCSiNB-I in Fig. 2(a) is studied. The DCSiNB-II also shows a plateau in the force–displacement curve [Fig. S2(a) in the supplementary material]. The corresponding straight Si beam with thickness of 21.72 and length of 47.8 Å is studied for comparison. The temperature profiles and heat flux of DCSiNB-II are calculated in Fig. S5 in the supplementary material. As shown in Fig. 3(b), DCSiNB-II without deformation ($D_x = 0.0$ Å) can cause 28.6% reduction of σ compared with the straight Si beam. Similar as the DCSiNB-I, the deformed DCSiNB-II

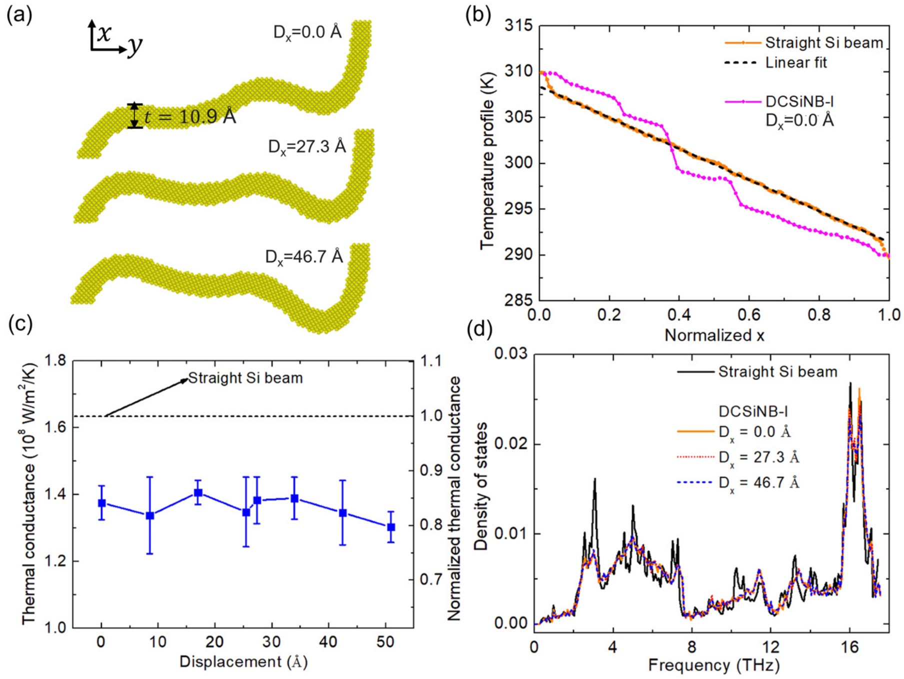

FIG. 2. (a) The DCSiNB-I without deformation ($D_x = 0.0$) and deformed DCSiNB-I with $D_x = 27.3$ and 46.7 Å in the $-x$ direction. (b) Temperature profile of the DCSiNB-I with $D_x = 0$ Å and the corresponding straight Si beam along the x direction. The black dashed line is the linear fit for the straight Si beam. (c) Thermal conductance of the deformed DCSiNB-I with displacement from 0 to 51 Å at 300 K. The dashed line is for the corresponding straight Si beam without compression. (d) Phonon density of states of straight Si beam and the DCSiNB-I with $D_x = 0$, 27.32, and 46.67 Å.

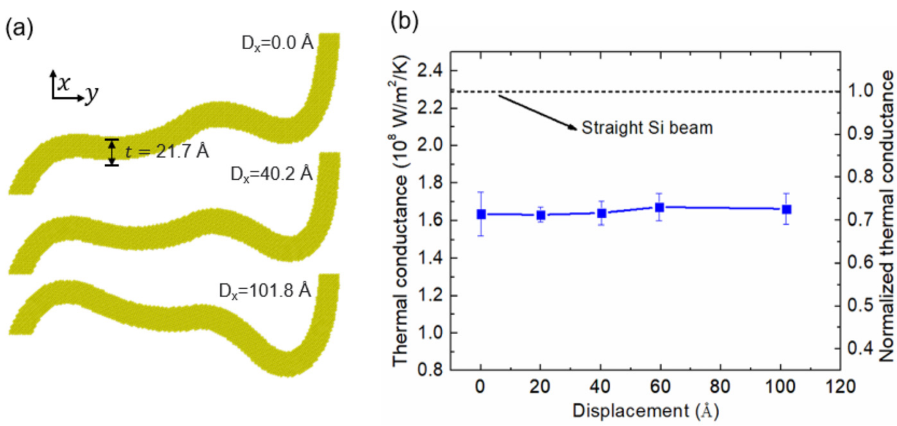

FIG. 3. (a) The structure of DCSiNB with thickness of 21.7 Å (denoted as DCSiNB-II). The deformed DCSiNB-II with $D_x = 0.0$, 40.2, and 101.8 Å in the $-x$ direction are shown. The DCSiNB-II doubles the size of DCSiNB-I in Fig. 2(a). (b) Thermal conductance of the deformed DCSiNB-II vs displacement at 300 K. The σ of the corresponding straight Si beam (black dashed line) is shown for comparison.

also has almost unchanged σ as the displacement increases, which further confirms the deformation insensitive σ of the designed Si metamaterial.

To further understand the deformation insensitive σ, the local stress in the deformed DCSiNB-I with $D_x = 0$, 27.32, and 46.67 Å are calculated by LAMMPS.[34] The value of the local stress is according to the color bars. Figure 4(a) shows that only the locations with larger curvature have relatively larger local stress, while most parts have a small value of local stress in DCSiNB-I. Furthermore, Fig. 4(b) shows that the average values of local stress (σ_{xx}, σ_{yy}, and σ_{zz}) of the three sections [S1–S3 in Fig. 4(a)] are ultra-small (<151 MPa) compared with the stress of bulk Si with strain $= -0.5\%$,[38] Si nanowire with strain $= 1\%$,[24] and the bent Si nanowire[21] at half diameter region. Consequently, a large deformation just causes a small local stress in DCSiNB-I, which in turn leads to the deformation insensitive σ.

With the development of nanotechnology, the nanostructures can be fabricated to several nanometers.[39–43] For example, the thickness of the ultra-thin hydrogenated amorphous silicon films can be reduced to 3.4 nm,[39] the diameter of nanowires can be fabricated to as small as 2[41] and 1.3 nm.[40] To verify whether the Si nanobeam with thickness capable of experimental fabrication can preserve the thermal properties and mechanical properties, Si nanobeam with thickness of 3.26 and 4.34 nm are further studied with the same settings as that in Fig. 2. The structure of DCSiNBs with thickness of 3.26 and 4.34 nm are in Figs. 5(a) and 5(b), respectively. As shown in Fig. 5(c), the thermal conductance of these DCSiNBs is also insensitive to the deformation. In addition, their force-displacement curves vs displacement are added in Fig. S8 in the supplementary material. Therefore, the thicker DCSiNBs, which could be expected experimentally fabricated, can have the same trend of thermal properties and mechanical properties as the thinner one in Fig. 2.

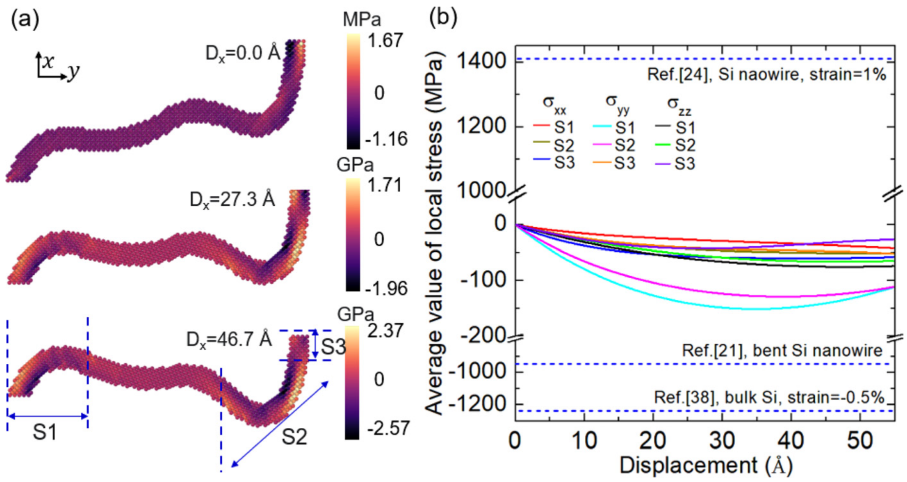

FIG. 4. (a) Local stress (σ_{xx}) distribution in DCSiNB-I without deformation ($D_x = 0$ Å) and with deformations ($D_x = 27.32$ and 46.67 Å). The value of the local stress is according to the color bars. (b) Average value of local stress in sections 1–3 (denoted as S1–S3). The dashed blue lines correspond to the stress in bulk Si with strain = −0.5%,[38] bent Si nanowire,[21] and Si nanowire with strain = 1%.[24] The averaged local stress is ultra-small compared with that in bulk Si and Si nanowire.

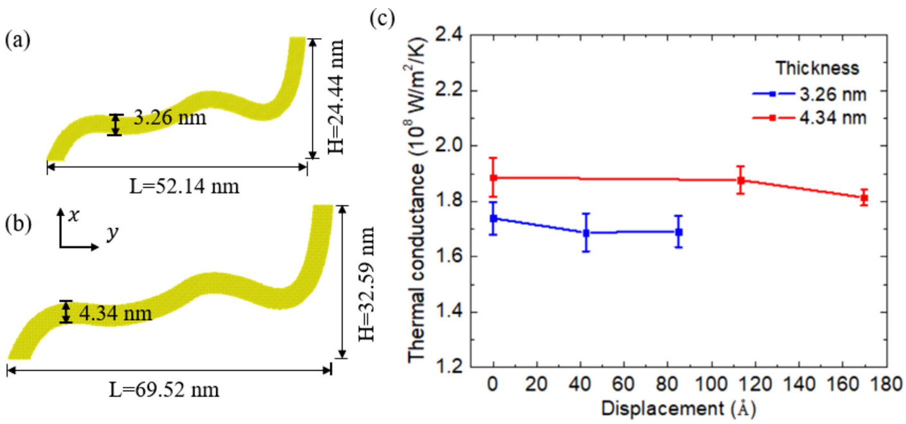

FIG. 5. The structure of DCSiNBs with thickness of 3.26 nm (a) and 4.34 nm (b). The size of the DCSiNB with thickness of 3.26 nm (4.34 nm) is 52.14 nm (69.52 nm) and 24.44 nm (32.59 nm) in y and x directions, respectively. (c) The thermal conductance of DCSiNBs with thickness of 3.26 and 4.34 nm at 300 K vs displacement.

In this work, the designed Si metamaterial built with DCSiNBs is investigated by NEMD simulations. Interestingly, the σ of the designed Si metamaterial is insensitive to large deformation (strain of −41%). The thermal transport behavior of the designed Si metamaterial is determined by DCSiNB, which has QZS feature. Further study confirms that there is an almost unchanged σ of DCSiNB under deformation. Under large deformation, the DOS of DCSiNB is little changed, and the average value of local stress is ultra-small, which can lead to the deformation insensitive σ. In addition, compared with the corresponding straight Si beam, the DCSiNB can cause 28.6% reduction of σ. The results of this work are meaningful for the multifunctional applications of elaborately designed metamaterial with both unchanged thermal conductance and quasi-zero stiffness feature under deformation, such has both stable thermal and stable mechanical properties.

See the supplementary material for the details of creation of the designed Si metamaterial. The details of analyses of the force–displacement curves for different designed curved Si nanobeam, the phonon density of states, and the temperature distribution of the designed curved Si nanobeam are also shown in the supplementary material. The designed curved Si nanobeam with thicknesses of 3.26 and 4.34 nm and NEMD results using two unit cells of the designed Si metamaterial are also studied in the supplementary material.

This work was sponsored by the National Natural Science Foundation of China (Grant No. 12004033) (L.Y.), the National Key Research and Development Project of China, No. 2018YFE0127800, the Fundamental Research Funds for the Central Universities, No. 2019kfyRCPY045 (N. Yang), and National Natural Science Foundation of China (Grant No. 12002030) (Q.Z.). The authors thank the National Supercomputing Center in Tianjin (NSCC-TJ) and the China Scientific Computing Grid (ScGrid) for providing assistance in computations.

AUTHOR DECLARATIONS

Conflict of Interest

The authors have no conflicts to disclose.

Author Contributions

Lina Yang: Conceptualization (equal); Data curation (equal); Formal analysis (equal); Investigation (equal); Methodology (equal); Project administration (equal); Validation (equal); Visualization (equal);

Writing – original draft (equal); Writing – review & editing (equal). **Quan Zhang:** Conceptualization (equal); Visualization (equal). **Gengkai Hu:** Conceptualization (equal); Visualization (equal). **Nuo Yang:** Conceptualization (equal); Data curation (equal); Formal analysis (equal); Investigation (equal); Methodology (equal); Project administration (equal); Supervision (equal); Visualization (equal); Writing – original draft (equal); Writing – review & editing (equal).

DATA AVAILABILITY

The data that support the findings of this study are available from the corresponding author upon reasonable request.

REFERENCES

[1]A. Vyatskikh, S. Delalande, A. Kudo, X. Zhang, C. M. Portela, and J. R. Greer, "Additive manufacturing of 3D nano-architected metals," Nat. Commun. **9**(1), 593 (2018).
[2]L. R. Meza, S. Das, and J. R. Greer, "Strong, lightweight, and recoverable three-dimensional ceramic nanolattices," Science **345**, 1322 (2014).
[3]J. Bauer, A. Schroer, R. Schwaiger, and O. Kraft, "Approaching theoretical strength in glassy carbon nanolattices," Nat. Mater. **15**, 438 (2016).
[4]N. G. Dou, R. A. Jagt, C. M. Portela, J. R. Greer, and A. J. Minnich, "Ultralow thermal conductivity and mechanical resilience of architected nanolattices," Nano Lett. **18**, 4755 (2018).
[5]J.-K. Yu, S. Mitrovic, D. Tham, J. Varghese, and J. R. Heath, "Reduction of thermal conductivity in phononic nanomesh structures," Nat. Nanotechnol. **5**, 718 (2010).
[6]M. Maldovan, "Phonon wave interference and thermal bandgap materials," Nat. Mater. **14**, 667 (2015).
[7]L. Yang, N. Yang, and B. Li, "Extreme low thermal conductivity in nanoscale 3D Si phononic crystal with spherical pores," Nano Lett. **14**, 1734 (2014).
[8]B. L. Davis and M. I. Hussein, "Nanophononic metamaterial: Thermal conductivity reduction by local resonance," Phys. Rev. Lett. **112**, 055505 (2014).
[9]M.-S. Pham, C. Liu, I. Todd, and J. Lertthanasarn, "Damage-tolerant architected materials inspired by crystal microstructure," Nature **565**, 305 (2019).
[10]Q. Zhang, D. Guo, and G. Hu, "Tailored mechanical metamaterials with programmable quasi-zero-stiffness features for full-band vibration isolation," Adv. Funct. Mater. **31**, 2101428 (2021).
[11]L. Yang, D. Huh, R. Ning, V. Rapp, Y. Zeng, Y. Liu, S. Ju, Y. Tao, Y. Jiang, J. Beak, J. Leem, S. Kaur, H. Lee, X. Zheng, and R. Prasher, "High thermoelectric figure of merit of porous Si nanowires from 300 to 700 K," Nat. Commun. **12**(1), 3926 (2021).
[12]X. Qian, J. Zhou, and G. Chen, "Phonon-engineered extreme thermal conductivity materials," Nat. Mater. **20**, 1188 (2021).
[13]C. Portela and J. Ye, "Architectures down to nano," Nat. Mater. **20**, 1451 (2021).
[14]B. Tian, P. Xie, T. J. Kempa, D. C. Bell, and C. M. Lieber, "Single-crystalline kinked semiconductor nanowire superstructures," Nat. Nanotechnol. **4**, 824 (2009).
[15]Q. Zhang, Z. Cui, Z. Wei, S. Y. Chang, L. Yang, Y. Zhao, Y. Yang, Z. Guan, Y. Jiang, and J. Fowlkes, "Defect facilitated phonon transport through kinks in boron carbide nanowires," Nano Lett. **17**, 3550 (2017).
[16]L. Yang, R. Prasher, and D. Li, "From nanowires to super heat conductors," J. Appl. Phys. **130**, 220901 (2021).
[17]J.-W. Jiang, N. Yang, B.-S. Wang, and T. Rabczuk, "Modulation of thermal conductivity in kinked silicon nanowires: Phonon interchanging and pinching effects," Nano Lett. **13**, 1670 (2013).
[18]Y. Zhao, L. Yang, C. Liu, Q. Zhang, Y. Chen, J. Yang, and D. Li, "Kink effects on thermal transport in silicon nanowires," Int. J. Heat Mass Transfer **137**, 573 (2019).
[19]L. Yang, Q. Zhang, Z. Wei, Z. Cui, Y. Zhao, T. T. Xu, J. Yang, and D. Li, "Kink as a new degree of freedom to tune the thermal conductivity of Si nanoribbons," J. Appl. Phys. **126**, 155103 (2019).
[20]L.-C. Liu, M.-J. Huang, R. Yang, M.-S. Jeng, and C.-C. Yang, "Curvature effect on the phonon thermal conductivity of dielectric nanowires," J. Appl. Phys. **105**, 104313 (2009).
[21]X. Liu, H. Zhou, G. Zhang, and Y.-W. Zhang, "The effects of curvature on the thermal conduction of bent silicon nanowire," J. Appl. Phys. **125**, 082505 (2019).
[22]Y. Liu, K. He, G. Chen, W. R. Leow, and X. Chen, "Nature-inspired structural materials for flexible electronic devices," Chem. Rev. **117**, 12893 (2017).
[23]D.-Y. Khang, H. Jiang, Y. Huang, and J. A. Rogers, "A stretchable form of single-crystal silicon for high-performance electronics on rubber substrates," Science **311**, 208 (2006).
[24]H. Zhang, J. Tersoff, S. Xu, H. Chen, Q. Zhang, K. Zhang, Y. Yang, C.-S. Lee, K.-N. Tu, and J. Li, "Approaching the ideal elastic strain limit in silicon nanowires," Sci. Adv. **2**, e1501382 (2016).
[25]A. R. Abramson, C.-L. Tien, and A. Majumdar, "Interface and strain effects on the thermal conductivity of heterostructures: A molecular dynamics study," J. Heat Transfer **124**, 963 (2002).
[26]Y. Kuang, L. Lindsay, S. Shi, X. Wang, and B. Huang, "Thermal conductivity of graphene mediated by strain and size," Int. J. Heat Mass Transfer **101**, 772 (2016).
[27]Q. Wang, L. Han, L. Wu, T. Zhang, S. Li, and P. Lu, "Strain effect on thermoelectric performance of InSe monolayer," Nanoscale Res. Lett. **14**(1), 287 (2019).
[28]B. Ding, X. Li, W. Zhou, G. Zhang, and H. Gao, "Anomalous strain effect on the thermal conductivity of low-buckled two-dimensional silicene," Natl. Sci. Rev. **8**, nwaa220 (2021).
[29]Z. Yang, R. Feng, F. Su, D. Hu, and X. Ma, & Nanostructures. "Isotope and strain effects on thermal conductivity of silicon thin film," Physica E **64**, 204 (2014).
[30]X. Li, K. Maute, M. L. Dunn, and R. Yang, "Strain effects on the thermal conductivity of nanostructures," Phys. Rev. B **81**, 245318 (2010).
[31]M. Alam, M. P. Manoharan, M. A. Haque, C. Muratore, and A. Voevodin, "Influence of strain on thermal conductivity of silicon nitride thin films," J. Micromech. Microeng. **22**, 045001 (2012).
[32]D. Fan, H. Sigg, R. Spolenak, and Y. Ekinci, "Strain and thermal conductivity in ultrathin suspended silicon nanowires," Phys. Rev. B **96**, 115307 (2017).
[33]K. F. Murphy, B. Piccione, M. B. Zanjani, J. R. Lukes, and D. S. Gianola, "Strain-and defect-mediated thermal conductivity in silicon nanowires," Nano Lett. **14**, 3785 (2014).
[34]A. P. Thompson, H. M. Aktulga, R. Berger, D. S. Bolintineanu, W. M. Brown, P. S. Crozier, P. J. in't Veld, A. Kohlmeyer, S. G. Moore, and T. D. Nguyen, "LAMMPS – A flexible simulation tool for particle-based materials modeling at the atomic, meso, and continuum scales," Comput. Phys. Commun. **271**, 108171 (2022).
[35]F. H. Stillinger and T. A. Weber, "Computer simulation of local order in condensed phases of silicon," Phys. Rev. B **31**, 5262 (1985).
[36]J. Chen, G. Zhang, and B. Li, "Molecular dynamics simulations of heat conduction in nanostructures: Effect of heat bath," J. Phys. Soc. Jpn. **79**, 074604 (2010).
[37]J. D. Gale and A. L. Rohl, "The general utility lattice program (GULP)," Mol. Simul. **29**, 291 (2003).
[38]V. Kuryliuk, O. Nepochatyi, P. Chantrenne, D. Lacroix, and M. Isaiev, "Thermal conductivity of strained silicon: Molecular dynamics insight and kinetic theory approach," J. Appl. Phys. **126**, 055109 (2019).
[39]Y. Abdulraheem, I. Gordon, T. Bearda, H. Meddeb, and J. Poortmans, "Optical bandgap of ultra-thin amorphous silicon films deposited on crystalline silicon by PECVD," AIP Adv. **4**, 057122 (2014).
[40]D. Ma, C. Lee, F. Au, S. Tong, and S. Lee, "Small-diameter silicon nanowire surfaces," Science **299**, 1874 (2003).
[41]P. Gentile, T. David, F. Dhalluin, D. Buttard, N. Pauc, M. Den Hertog, P. Ferret, and T. Baron, "The growth of small diameter silicon nanowires to nanotrees," Nanotechnology **19**, 125608 (2008).
[42]R. A. Puglisi, C. Bongiorno, S. Caccamo, E. Fazio, G. Mannino, F. Neri, S. Scalese, D. Spucches, and A. La Magna, "Chemical vapor deposition growth of silicon nanowires with diameter smaller than 5 nm," ACS Omega **4**, 17967 (2019).
[43]S. Gao, S. Hong, S. Park, H. Y. Jung, W. Liang, Y. Lee, C. W. Ahn, J. Y. Byun, J. Seo, and M. G. Hahm, "Catalyst-free synthesis of sub-5 nm silicon nanowire arrays with massive lattice contraction and wide bandgap," Nat. Commun. **13**, 3467 (2022).